Lithium Diffusion in Li_xCoO_2 Electrode Materials

Gerhard Nuspl,# Masataka Nagaoka, Kazunari Yoshizawa,† Fumihito Mohri, and Tokio Yamabe*

Institute for Fundamental Chemistry, 34-4 Takano-Nishihiraki-cho, Sakyo-ku, Kyoto 606-8103

†Department of Molecular Engineering, Kyoto University, Sakyo-ku, Kyoto 606-8501

(Received December 1, 1997)

The minimum energy migration path and the minimum barrier height of lithium diffusion are discussed for the layer compound Li_xCoO_2. The Universal Force Field (UFF) is adapted for use in solid state compounds. Molecular dynamics simulations with additional impulse dynamics method, performed at a microcanonical ensemble, point out that the lithium migration between the Co–O octahedron layers takes place by ion hopping from one octahedral to another octahedral site via an interstitial tetrahedral site. The barrier height of lithium migration is estimated to be 28.7 kJ mol^{-1} (0.30 eV) for an original layer distance of 2.54 Å; a potential energy profile is developed from molecular mechanics calculations. The observation that the repulsive van der Waals interaction between Li^+ and neighboring O^{2-} ions is the most important contribution to the barrier height is consistent with the fact that the activation energy of lithium diffusion is very sensitive to the layer distance, within the experimentally observed values.

In the last two decades, an uncountable number of various insertion compounds have been investigated with respect to their use as possible electrode materials in rechargeable lithium ion batteries.[1—4] Such kinds of ion batteries are interesting for backup use in computer memories, for example. In particular, transition metal oxides[5—12] and chalcogenides[5—7,13—17] consisting of layer structures or three-dimensional frameworks with tunnel systems insert remarkable amounts of lithium.

Up to now, for consumer applications the most promising cathode material for solid state lithium ion batteries is Li_xCoO_2,[18,19] since this compound shows a high theoretical energy density of 766 W h kg^{-1}.[1] The use of Li_xCoO_2 in commercial lithium ion batteries[20] has initiated intensive research efforts in this field.[1,12—27] Recently, beside the original lithium ion battery[20,28—30] including a Li_xCoO_2 cathode and an amorphous carbon anode, many so-called "rocking chair" cells in which both electrodes are lithium intercalation compounds are under development. One important example of these new types of cells consists of nanostructured TiO_2 (anatase) as the anode and $LiCoO_2$ or $LiNi_{0.5}Co_{0.5}O_2$ as the cathode.[22]

Li_xCoO_2, isostructural with the α-$NaFeO_2$ structure type, is a typical layer compound formed by stacking sheets consisting of CoO_6 octahedra. The octahedra in one layer share six edges each, resulting in a stoichiometry of CoO_2 within one octahedron layer. The stacking sequence of the CoO_2 layers is ABCABC, leading to a trigonal unit cell with space group $R\bar{3}m$. Therefore, Li_xCoO_2 can also be regarded as a filled derivative of the $CdCl_2$ structure type. The empty octahedral sites between the CoO_2 layers are statistically likely to be occupied with lithium ions. The crystal structure of Li_1CoO_2, also adopted in $LiVO_2$,[31,32] $LiCrO_2$,[33] and $LiNiO_2$,[34,35] is shown in Fig. 1 (hexagonal axes).

Interestingly, the distance between the MO_2 octahedron layers is larger in Li_xCoO_2 than in the other $LiMO_2$ oxides. This fact is regarded as an important reason why a higher Li^+ mobility is observed in Li_xCoO_2 than in the other oxides.[18] Recently CoO_2, the end member of the Li_xCoO_2 solid solution, was also characterized by in situ X-ray diffraction in an electrochemical cell by complete lithium deintercalation.[36] Even so, the technologically interesting region of lithium

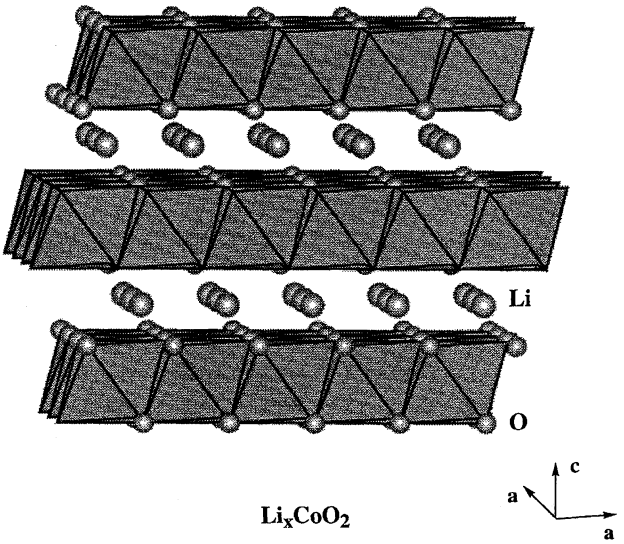

Fig. 1. Crystal structure of the layer compound Li_xCoO_2 ($0.5 < x < 1$). All possible sites of lithium insertion are shown (Li_1CoO_2). For lower lithium contents, the same sites are occupied statistically.

Present address: Institut für Anorganische Chemie der LMU München, Meiserstr. 1, D-80333 München, Germany.

insertion lies between 0.5 and 0.9 Li/Ti.

The diffusion in Li_xCoO_2 has been carefully investigated as to dependency on stoichiometry using the electrochemical voltage spectroscopy. Barker et al.[37] reported the average diffusion coefficient for the composite Li_xCoO_2 cathode to be in the range of 10^{-9} cm^2 s^{-1}, which indicates a relatively facile reaction kinetics for the lithium insertion reaction. Our purpose is to explain these results microscopically from a theoretical point of view. A detailed analysis of lithium and sodium diffusion in the natural mineral TiO_2 anatase has been published by comparing quantum chemical ab initio periodic Hartree–Fock and modified semiempirical INDO calculations with experimental electrochemical measurements.[38] In the present work, we have chosen another way to explore the nature of lithium diffusion in Li_xCoO_2 using theoretical methods. Our approach is based on force field simulations which allow the investigation of solid state structures with large unit cells. For this reason the Universal Force Field (UFF)[39] has been adapted for its use in solid state compounds.

Computational Details

The lithium diffusion path in Li_xCoO_2 and the activation energy of lithium migration were investigated using the *Cerius*^{2} program package.[40] The UFF,[39] a full periodic table force field for general purposes, is used in all molecular mechanics (MM) and molecular dynamics (MD) simulations. The force field parameters implemented in *Cerius*^{2} are derived from general rules based on the element, its hybridization and connectivity. Partial charges of Li, Co, and O were obtained from the charge equilibrium method[41] recommended for use in conjunction with the UFF. Coulomb interactions and the dispersive part of the van der Waals interactions are calculated with the Ewald summation procedure[42,43] described in a new approach for accelerated convergence by Karasawa and Goddard, III.[44] A Lennard Jones 12—6 potential was chosen as a representation of the van der Waals interaction.

Since the accuracy of every MM or MD simulation is strongly dependent on the quality of the force field used for each special purpose, several possibilities have been tested in this work. It was our purpose to retain the general character of the UFF and to avoid a loss of this generality by a mathematical fitting of input parameters. For the simulation of the periodic properties of Li_xCoO_2, the following use of the UFF has shown to be most physically plausible and reasonable. Valence terms are explicitly calculated for the Co–O bonds and O–Co–O or O–Co–O angles. Because of the high ionic character of the inserted lithium ions, Li–O and Li–Co interactions are treated as nonbonding interactions (van der Waals and Coulombic interactions only).

The charge equilibrium method[41] results in a partial charge of +1.0 for Li in $LiCoO_2$, supporting the expected high ionic character. Mulliken population analyses using the extended Hückel crystal orbital method[45,46] indicate a similar high ionic character (+1.05) of lithium for the lithium intercalation in anatase ($Li_{0.5}TiO_2$).[47] Since in the UFF no input parameter set is available for oxygen in a crystal octahedral environment, the parameter set of oxygen in a trigonal environment was adjusted for our model in the following way: According to Shannon's effective ionic radii set,[48] the "natural radius" of oxygen in the UFF was enlarged by 0.04 Å (difference in oxygen ionic radii between CN3 and CN6). The "natural angle" θ_0, one of the input parameters of the UFF and important for the calculation of the angular distortions, is set to an ideal octahedral environment for the O–Co–O and the Co–O–Co angles with $\theta_0 = 90°$. For Li and Co atoms, the tabulated parameters[41] for Li and Co^{3+} in an octahedral environment were chosen.

By fixing the experimental unit cell parameters the Co–O bond distances were optimized to be 1.947 Å in $LiCoO_2$ when performing an energy minimization of one unit cell using periodic boundary conditions. For the isotypic compound $LiNiO_2$, an experimental Ni–O bond length of 1.926 Å was reported.[35]

Migration Path of the Lithium Ions in Li_xCoO_2

Let us first look at where local energy minima and the transition state are located for the Li^+ ion while hopping from one octahedral site to another empty octahedral site. In order to determine the energetically most favorable diffusion path of Li^+, MD simulations were performed. However, in comparison to the diffusion of atoms in liquids, the diffusion in solids is very slow.[49,50] Usually by far the majority of the atoms in a crystalline solid are merely vibrating in the vicinity of their equilibrium positions without hopping to another site. The number of jumps Γ to a neighboring site out of ν vibrations made by the atom per second is

$$\Gamma = \nu \exp(-Q_a/k_B T), \quad (1)$$

where Q_a is the activation energy per atom.[48] Therefore, only one out of all the many million vibrations that each atom carries out every second will lead to a successful hopping to a neighboring site, either because of a large amplitude of the vibration or because of a fortuitous correlation with the motion of its neighbors.[48,49] This fact shows an important consequence for MD simulations: Usually the simulation box containing 1000 to 1500 atoms and the simulation time (about 5 to 15 ps) are too small to observe a direct hopping of atoms in a neighboring site. This is also true for the motion of the Li^+ ions between the octahedron layers in Li_xCoO_2. The Li^+ ions are trapped at the octahedral sites and only a thermal motion (Debye Waller type thermal motion) of the Li^+ ions should be observed by usual MD simulations. This behavior is independent of the chosen dynamics method, whether it might be the constant NVE or NPT dynamics, in which either the number of atoms (N), the volume (V), the energy (E) or N, the pressure (P) and the temperature (T) are held constant.

One possibility for avoiding such a problem in MD simulations was suggested for the lithium diffusion in silicate glasses.[51] The basic idea of this approach is to share the momentum among different kinds of atoms. An extra momentum is added to the Li^+ ions, allowing a larger movement

in a shorter time, while the remaining lattice is relaxing at the desired temperature. Because of the higher regularity of the Li_xCoO_2 lattice in comparison to amorphous silicate glasses, a strongly modified method using the "impulse dynamics" (ID) tool of the *Cerius*[2] simulation module is developed in this work. However, ID is restricted to the microcanonical (constant NVE) ensemble.

The simulation box shown in Fig. 2 contains 901 atoms, which corresponds to 100 unit cells of $LiCoO_2$ (300 cobalt, 600 oxygen and 1 lithium). The dimension and the initial configuration of the simulation box are based on the observed unit cell parameters for $LiCoO_2$.[7,18,19] First, only the (idealized) CoO_2 octahedron layers are taken and one lithium ion is inserted at an arbitrary octahedral site (0.555, 0.5277, 1/3) of the box. We will explain later why this simplified model is the best assumption for the following ID simulation. After charge equilibration, and after the initial velocities are assigned with a Maxwell–Boltzmann distribution, the lattice is equilibrated in an NVE ensemble for 5 ps (5000 time steps of 0.001 ps each) to the target temperature of 300 K by applying velocity scaling. Then the system is further allowed to relax at 300 K for 10 ps (10000 steps) without velocity scaling.

During relaxation, the Li^+ ion is trapped in its octahedral site, as mentioned above. If the Li^+ ion is placed at an arbitrary site within the Co–O octahedron layers before starting the MD simulation, it will move to the next neighboring empty octahedral site within the first 50 to 100 time steps. Again, only a thermal movement of the Li^+ ion is observed after several hundred time steps because the ion transfers its surplus energy to the host lattice.

After relaxation of the lattice for 1.5 ps (15000 time steps), the Li^+ ions are "shot" in different directions in order to find the minimum energy pathway of migration. For this reason, a directional velocity with known value is added to the lithium ion and a further MD simulation run is performed for 100 to 200 time steps of 0.001 ps each (0.1 to 0.2 ps as a whole). The velocities of the surrounding lattice are assigned from the usual Maxwell–Boltzmann distribution. During the MD simulation run, the lattice was allowed to relax. If the chosen energy of the Li^+ ion, which is easily calculated by $\Delta E = 1/2 m_{Li} v^2$, is high enough, the Li^+ ion will pass over the barrier height of hopping and will migrate to a neighboring octahedral site, usually within 0.1 ps. By trial and error and by testing about 30 different directions or trajectories, the minimum energy pathway of lithium migration can be determined, as illustrated in Fig. 3. Now the lattice is shown in the direction of the *c*-axis.

With lower velocities of 40 to 60 $Å\,ps^{-1}$, which correspond to an energy region of 0.58 to 1.30 eV, the Li^+ ion is trapped at once after one hopping to a neighboring octahedral site and the surplus energy is transferred to the surrounding lattice. Only with very high initial velocities, about 100 $Å\,ps^{-1}$ or an energy of 3.6 eV, is a further migration of the Li^+ ion observed, as shown in the following example of a performed simulation. The Li^+ ion migrates over twelve sites, before it is finally trapped. Always the migration continues by hopping via an interstitial tetrahedral site. It has not been observed that the direct way between octahedral sites is chosen. Additionally, also a direct hopping from interstitial tetrahedral site to a neighboring interstitial tetrahedral site is observed (step 4 in Fig. 4). Of course, in reality, such high energies and velocities of a single atom are very unlikely at 300 K and in fact, such a long migration will not occur in short observation times at room temperature. Nevertheless, the results show that ID is a valuable tool for a general study of diffusion processes and migration pathways in certain solids. Even for solid state compounds the disadvantage of comparatively small simulation boxes and short calculation times can be partly overcome by using the ID

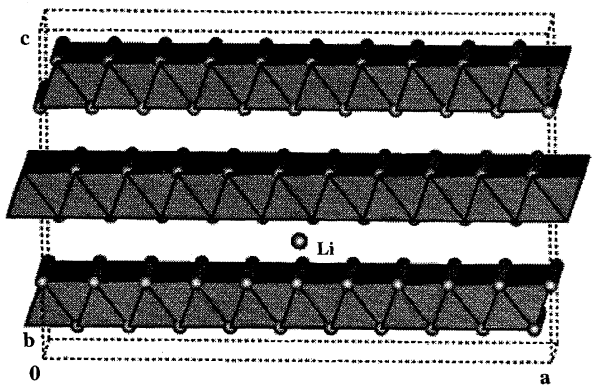

Fig. 2. Simulation box for MD simulations using the UFF (NVE ensemble). The box totally contains 901 atoms (300 cobalt, 600 oxygen and 1 lithium) which corresponds to 100 unit cells of Li_xCoO_2.

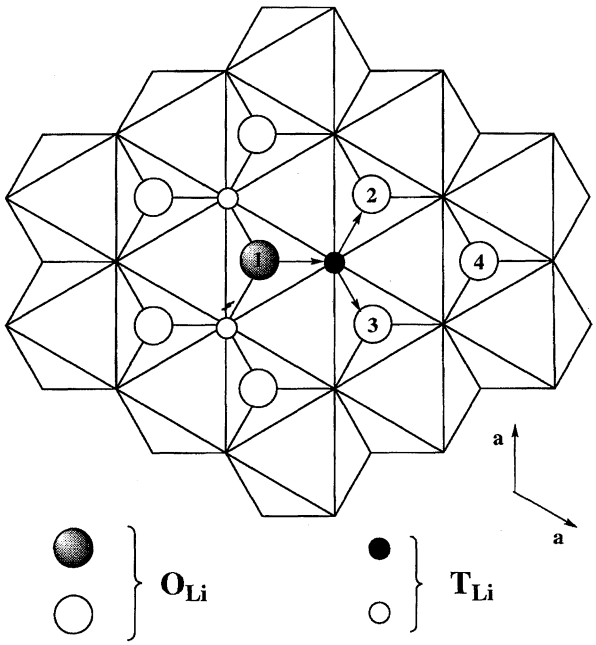

Fig. 3. Minimum energy pathway of lithium migration from a regular octahedral site O_{Li} to a neighboring octahedral site O_{Li} via an interstitial tetrahedral site T_{Li}.

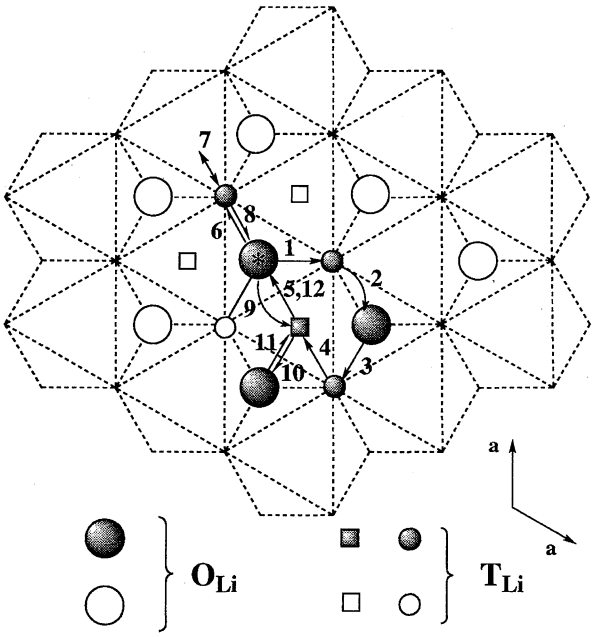

Fig. 4. Pathway of a migrating Li^+ ion by adding a high momentum in [210] direction (3.6 eV). The initial state is marked with a star and the Li^+ is hopping in direction of the arrows form octahedral site to tetrahedral site. Step 4 also shows a direct hopping from T_{Li} to T_{Li}. After about 0.8 to 1.0 ps the Li^+ is vibrating around the initial position, again.

tool. During the migration from one octahedral site to another octahedral site, the layer distance increases distinctly at the present position of the Li^+ ion. This characteristic behavior of lithium diffusion in Li_xCoO_2 is examined in detail in the next chapter.

The minimum energy migration path via an interstitial tetrahedral site shown in Fig. 3 leads to some general conclusions about the nature of lithium diffusion. From an inspection of Fig. 3 one can show that a hopping is energetically much more favorable if at least two neighboring octahedral sites, which are next to the interstitial tetrahedral site (marked as **2** and **3** in Fig. 3), are vacant. If one of the two sites is occupied by an additional Li^+ ion, repulsive Coulombic and van der Waals Li^+–Li^+ interactions increases drastically, since the distance between a regular octahedral and an interstitial tetrahedral site is only 1.7 Å. Therefore, the barrier height increases by orders of magnitudes, which is also supported by MD simulations using the ID tool. If the Li^+ ion is "shot" in direction of the interstitial tetrahedral site, a neighboring Li^+ ion located in position **2** or **3** of Fig. 3 is catapulted away from its equilibrium position like a ball in a billiard game. A neighboring Li^+ ion in position **4** shows a similar but weaker influence.

We are aware that such correlation effects between neighboring Li^+ ions may also play an important role in the Li^+ diffusion in Li_xCoO_2. However, to our experience, at the present stage the possible size of a simulation box is by far too small to include such effects in a quantitative way in MD simulations; consequently simplifications are necessary. Therefore, out of many tested possibilities and different stoichiometries like $Li_{0.5}CoO_2$, $Li_{0.75}CoO_2$, and $Li_{0.9}CoO_2$ for example, the choice of a simulation box containing the CoO_2 layers and only one additional Li^+ has shown to be the best compromise for our purpose. In all MD calculation using the above-mentioned examples, the Li^+ migration takes place from an octahedral site to a neighboring octahedral site via an interstitial tetrahedral site. However, image effects caused by Li^+ ions leaving the box on one side and simultaneously entering the box as their image on the other side influence the applicability of these models which contain higher lithium contents. In particular, long range correlation effects between lithium ions cannot be observed in a realistic way. Such image effects could only be avoided by distinct larger simulation boxes which are beyond the possibilities of our present computer size and memory. Therefore we must restrict ourselves to a simpler model by omitting long range correlation effects between neighboring Li^+ ions. Even so, this simplified model represents the correct migration pathway since the pathway is mainly determined by the neighboring oxygen atoms. In other words, the Co–O framework plays a dominant role for the movement of the Li^+ ions within the layers. This aspect will be discussed in more detail in the next chapter.

In addition, the energy minimum pathway via an interstitial tetrahedral site obtained by ID simulations indicates that a local clustering of vacancies within the layers clearly improves the facility of lithium migration.

Activation Energy of Lithium Migration

With the knowledge of the minimum energy pathway, the barrier height of lithium migration can be estimated with MM calculations. Since there are no accurate experimental crystallographic data for Li_xCoO_2 containing fractional coordinates of lithium, cobalt, and oxygen, we assumed the following model: The experimental observed unit cell parameters of Li_1CoO_2 are fixed in all MM calculations and only the positions of the atoms within the unit cell are optimized by energy minimization techniques (Truncated Newton minimization).[40] Figure 5 (a) shows the unit cell of the optimized ground state model Li^OCoO_2, where the Li^+ is in an octahedral environment; in Fig. 5 (b), the optimized unit cell of the local minimum structure Li^TCoO_2 where Li^+ is in an interstitial tetrahedral site is shown.

In Fig. 5 (b), the Li^+ ion in the interstitial site is fixed at its position and the surrounding lattice is allowed to relax during optimization. The tetrahedral coordination is slightly distorted, with three longer Li–O distances of 1.984 Å and one shorter Li–O distance of 1.833 Å. The potential energy difference between an Li^+ in an octahedral (Fig. 5 (a)) and an Li^+ in a tetrahedral environment (Fig. 5 (b)) is calculated as 26.4 kJ mol^{-1} or 0.27 eV (see also Table 1). However, the layer distance between the Co–O octahedron layers increases by 0.43 Å from 2.54 Å for the Li^+ ion in an octahedral site to 2.97 Å, after placing one Li^+ into an interstitial tetrahedral site. Further investigations have shown that the repulsion

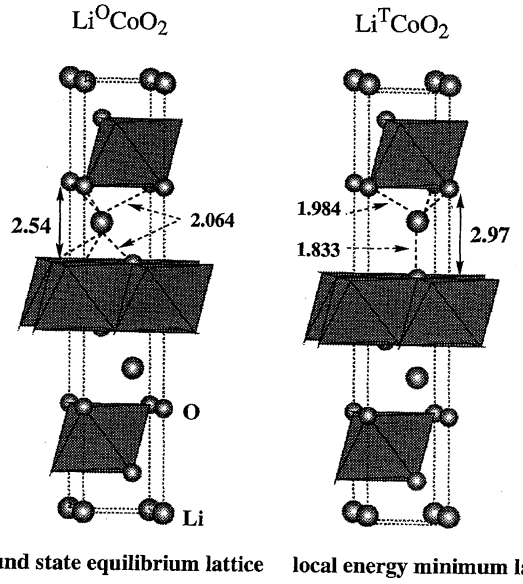

Fig. 5. Optimized unit cells of (a) ground-state equilibrium structure with the migrating Li^+ ion in an ideal octahedral environment and (b) local energy minimum structure with Li^+ in a slightly distorted tetrahedral environment. The Li^+ coordination is indicated with dashed lines.

Table 1. Comparison of the Energy Expression Terms (kJ mol^{-1}) Using the UFF after Lattice Relaxation for the Ground State Model Li^{O}CoO$_2$ and for the Local Minimum Structure Li^{T}CoO$_2$, Where One Li^+ Ion Is Fixed in an Interstitial Tetrahedral Site

	Li^{O}CoO$_2$	Li^{T}CoO$_2$
Valence terms:		
Bonds	39.62	33.60
Angles	24.18	31.34
Nonbonded Terms:		
Van der Waals term	41.73	69.21
Electrostatic term	−3274.59	−3276.85
Total energy[a)]	−3169.06	−3142.70

a) $\Delta E_{total}(Li^{O}CoO_2 - Li^{T}CoO_2) = 26.4$ kJ mol^{-1} (0.27 eV).

term of the van der Waals forces between the Li^+ ions and the neighboring O^{2-} ions are the most important contribution to the barrier height of lithium migration. This fact is also seen in Table 1. The major change of the potential energy appears in the van der Waals term. Surprisingly, changes in Coulombic interactions play a minor role for the lithium diffusion in the layer compound $LiCoO_2$, although they are by far the main contribution of the total energy.

In order to locate the transition state on the lithium migration path between an octahedral and an interstitial tetrahedral site, we fixed the relaxed lattice of the local energy minimum structure (Li^{T}CoO$_2$), then moved the Li^+ stepwise from the interstitial tetrahedral position in the direction of the octahedral position. We calculated the single potential energy of each intermediate geometry. The transition state is located at the point of intersection of the straight line from the octahedral to the interstitial tetrahedral site and the triangle face spanned by three oxygen ions of the LiO_4 tetrahedron. The geometry of the saddle point on the potential energy surface or the "bottleneck" of the lithium migration is shown in Fig. 6. The small black dot in Fig. 6 marks the lithium position of the transition state.

Since the "bottleneck" of lithium diffusion lies very close to the interstitial tetrahedral site, it is, in our opinion, reasonable for the estimation of the total energy barrier to keep the optimized structure of the local energetic minimum for the calculation of the transition state energy. In Fig. 7, the complete potential energy profile for the lithium migration via a tetrahedral site is shown. The total barrier height of lithium migration is estimated to be 28.7 kJ mol^{-1} or 0.30 eV. The fact that such a direct migration path between an octahedral and an interstitial tetrahedral site is energetically most favorable was confirmed by a dense mesh of single point energy

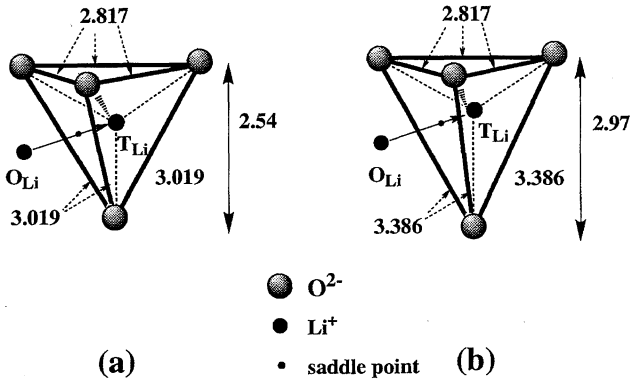

Fig. 6. Expansion of the oxygen ion triangle "bottleneck" during lithium migration from an octahedral to an interstitial tetrahedral site. The O^{2-}–O^{2-} interlayer distances (Å) and the layer distances (Å) are indicated for the (a) ground state equilibrium structure and the (b) energetic local minimum structure. The small black dot on the migration path arrow marks the position of the transition state.

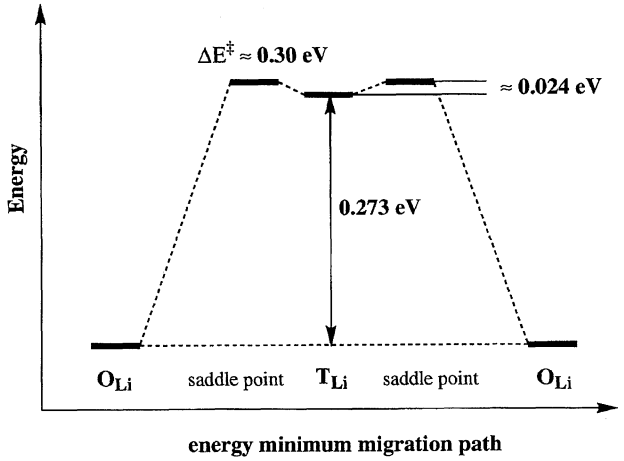

Fig. 7. Potential energy profile of lithium migration from a regular octahedral site O_{Li} to a neighboring octahedral site O_{Li} via an interstitial tetrahedral site T_{Li}.

calculations performed stepwise in all theoretical possible pathways. At first sight the existence of such a narrow bottleneck spanned by three oxygen ions would probably not be expected for such a layer structure, where the lithium ions seem to have much space for migration between the Co–O octahedron layers. In fact, the situation is not very different from three-dimensional systems containing narrow channels for insertion of small ions. The way of lithium migration is determined by a fixed migration path. However, in contrast to a framework lattice, a layer structure can more easily balance such stress by increasing the layer distance, whereas in a rigid three-dimensional framework it is much more difficult to enlarge the channel systems.

In order to demonstrate the dominant role of an enlargement of the layer distance between the Co–O octahedron layers during lithium diffusion, we performed the same MM calculations as above, but this time the surrounding lattice (and also the layer distance) of the optimized ground state structure (Li^OCoO_2) is fixed during lithium migration. Using the observed c-axis of 14.052 Å for $LiCoO_2$,[7] the total barrier height of lithium increases to 77.1 kJ mol^{-1} (0.8 eV) and the potential energy difference between the interstitial tetrahedral and the regular octahedral site is now calculated as 57.8 kJ mol^{-1} (0.6 eV). Of course, such a large barrier height of lithium migration is too high to allow the easy lithium diffusion necessary for a good electrode material like Li_xCoO_2. The reason for the drastically increasing high barrier height is the narrow bottleneck shown in Fig. 6 (b). Without lattice relaxation, the O^{2-}–O^{2-} interlayer distances would be only 3.019 Å and the intralayer O^{2-}–O^{2-} distance would be 2.817 Å.

Therefore, the MM calculations indicate that during lithium migration the narrow bottleneck must be distinctly stretched lowering the barrier height of lithium migration drastically. Whereas the intralayer O^{2-}–O^{2-} distance remains constant at 2.871 Å, the interlayer O^{2-}–O^{2-} distances increase to 3.386 Å after the lithium ion moved to the interstitial tetrahedral site. Since the repulsion energy part of the Lennard–Jones 12—6 function

$$E_{vdW} = D_0 \sum \left\{ [R_0/R]^{12} - [R_0/R]^6 \right\} \quad (2)$$

D_0 = well depth (kJ mol^{-1}),
R_0 = equilibrium van der Waals distance (pm)

increases to the 12th power with decreasing Li^+–O^{2-} distance, the layer distance must clearly increase during lithium migration in order to reduce strongly repulsive Li^+–O^{2-} van der Waals interactions.

Experimentally, a nearly linear increase in the *c*-axis from 14.052 to 14.42 Å is observed with decreasing lithium content in the region from $LiCoO_2$ to $Li_{0.49}CoO_2$.[36] If we simulate this observation in a simplified model by just enlarging the *c*-axis to 14.42 Å in our model structure, the total barrier height will decrease to 21.0 kJ mol^{-1} (0.22 eV) and the energy difference between the energetic ground state and local energetic minimum will be 19.3 kJ mol^{-1} (0.20 eV). Of course, this procedure is a first approximation to the real charging and discharging process since neither the change in the Li^+–Li^+ interactions nor the change in the cobalt oxidation state is taken into account. Further investigations are necessary to have a better understanding of the activation energy that should clearly depend on lithium content. However, our calculations indicate that the height of the activation barrier is mainly determined by the layer distance.

In addition, the Co–O octahedron layers remain nearly undistorted during lithium migration. In the ground equilibrium state Li^OCoO_2, all Co–O bonds are optimized to 1.947 Å and all O–Co–O bond angles to 92.7° or 87.3°. If the Li^+ is located in the interstitial site, the Co–O bond lengths will be 1.939 or 1.944 Å and the corresponding O–Co–O bond angles will be 92.8°, 93.0°, 93.2° and 87.2°, 87.0° and 86.8°, respectively.

Conclusions

MD simula tions are not only used as a valuable tool for the investigation of liquids and glasses, but also serves its purpose for the investigation of diffusion processes in certain solid-state compounds. However, due to the high regularity of solid compounds, modifications and simplifications of the original method are necessary. Therefore, the ID simulation tool available for the microcanonical ensemble has been used to develop the lithium energy minimum migration path in Li_xCoO_2. The simulations show that the lithium migration in Li_xCoO_2 takes place via an interstitial mechanism. The general method presented in this work should also be transferable to other insertion compounds containing layer or framework structures and can become especially important for such insertion compounds, where accurate crystallographic data are not available (like in Li_xCoO_2 itself). This is often the case for insertion compounds which are considered as possible electrode materials for lithium ion batteries because they usually show a high amorphous character and single crystals are often not available.

The MM calculations based on the UFF indicate that the barrier height of lithium migration is very sensitive to the local existing layer distance. Surprisingly, repulsive van der Waals, but not Coulombic interactions are the dominant contribution to the barrier height of lithium diffusion in Li_xCoO_2. As mentioned in the introduction, the lithium ions in Li_xCoO_2 are considered to be more mobile than in the other isotypic Li_xMO_2 oxides (M=V, Cr, Ni), owing to a larger layer distance. Our calculations support microscopically the experimental observation that the magnitude of the layer distance is very essential for the barrier height of lithium diffusion in layer compounds. Of course, an increasing layer distance is not only improving the lithium diffusion, but also destabilizing the lattice itself. Therefore, an increasing layer distance will always be in competition with other effects like stacking faults and arising of superstructures.

This work is part of a project of the Institute for Fundamental Chemistry supported by the "Research for the Future" Program of the Japan Society for the Promotion of Science

(JSPS-RFTF96P00206). G. N. is very grateful to the JSPS for generous financial support which enabled his stay at the Institute for Fundamental Chemistry. Moreover, this work was partly supported by the Carbon-Based Electronic Material Society (CBMS).

References

1) O. Yamamoto, in "Solid State Electrochemistry," ed by P. G. Bruce, Cambridge University Press, Cambridge (1995).
2) J. B. Goodenough, A. Manthiram, and B. Wnetrzewski, *J. Power Sources*, **43**, 269 (1993).
3) D. W. Murphy and P. A. Christian, *Science*, **205**, 651 (1979).
4) M. S. Whittingham, *Prog. Solid State Chem.*, **12**, 1 (1978).
5) W. R. Kinnon, in "Solid State Electrochemistry," ed by P. G. Bruce, Cambridge University Press, Cambridge (1995).
6) R. Brec, E. Prouzet, and G. Ouvrard, *J. Power Sources*, **43**, 277 (1993).
7) A. J. Jacobson, in "Solid State Chemistry Compounds," ed by A. K. Cheetham and P. Day, Clarendon Press, Oxford (1992).
8) H. Ohtsuka and J. Yamaki, *Solid State Ionics*, **35**, 201 (1989).
9) B. Zachau-Christiansen, K. West, T. Jacobsen, and S. Atlung, *Solid State Ionics*, **28**, 1176 (1988).
10) D. W. Murphy, P. A. Christian, F. J. Di Salvo, J. N. Carides, and J. V. Waszczak, *J. Electrochem. Soc.*, **128**, 2053 (1981).
11) D. W. Murphy, F. J. Di Salvo, J. N. Carides, and J. V. Waszczak, *Mater. Res. Bull.*, **13**, 1395 (1978).
12) J. J. Braconnier, C. Delmas, and P. Hagenmuller, *Mater. Res. Bull.*, **17**, 993 (1982).
13) J. R. Akridge and H. Vourlis, *Solid State Ionics*, **18/19**, 1082 (1986).
14) A. H. Thomson, *J. Electrochem. Soc.*, **126**, 608 (1979).
15) M. S. Whittingham and B. G. Silbernagel in "Solid Electrolyte," ed by W. van Gool and P. Hagenmuller, Academic Press, New York (1977).
16) M. S. Whittingham, *Science*, **192**, 1126 (1976).
17) J. O. Besenhard and R. Schöllhorn, *J. Power Sources*, **1**, 267 (1976).
18) K. Mizushima, P. C. Jones, P. J. Wiseman, and J. B. Goodenough, *Mater. Res. Bull.*, **15**, 783 (1980).
19) M. G. S. R. Thomas, P. G. Bruce, and J. B. Goodenough, *Solid State Ionics*, **17**, 13 (1985).
20) E. Mashiko, M. Yokokawa, and T. Nagaura, in "Extended Abstract of the 32nd Battery Symposium in Japan," Abstr., p. 31 (1991).
21) Y. Nishida, K. Nakane, and T. Satoh, in "Extended Abstract of the 8th Int. Meet. Lithium Batteries," Nagoya, Japan, Abstr., p. 440 (1996).
22) S. Huang, L. Kavan, I. Exnar, and M. Grätzel, *J. Electrochem. Soc.*, **142**, L142 (1995).
23) K. Brandt, *Solid State Ionics*, **69**, 173 (1994).
24) J. N. Reimers, E. W. Fuller, E. Rossen, and J. R. Dahn, *J. Electrochem. Soc.*, **140**, 3396 (1993).
25) T. Ohzuku, A. Ueda, and M. Nagayama, *J. Electrochem. Soc.*, **140**, 1862 (1993).
26) D. Guyomard and J. M. Tarascon, *J. Electrochem. Soc.*, **139**, 937 (1992).
27) J. R. Dahn, U. von Sacken, H. Al Janaby, and M. K. Juzkow, *J. Electrochem. Soc.*, **138**, 2207 (1991).
28) S. Yata, Y. Hato, H. Kinoshita, N. Ando, A. Anekawa, T. Hashimoto, M. Yamaguchi, K. Tanaka, and T. Yamabe, *Synth. Met.*, **73**, 273 (1995).
29) S. Yata, Kanebo Ltd., U. S. Patent 4601849 (July 1986).
30) K. Tanaka, K. Ohzeki, T. Yamabe, and S. Yata, *Synth. Met.*, **9**, 41 (1984).
31) L. A. de Piciotto, M. M. Thackeray, W. David, P. G. Bruce, and J. B. Goodenough, *Mater. Res. Bull.*, **19**, 1497 (1984).
32) L. A. Piciotto and M. M. Thackeray, *Mater. Res. Bull.*, **20**, 187 (1985).
33) S. Miyazaki, S. Kikkawa, and M. Koizumi, *Synth. Met.*, **6**, 211 (1983).
34) J. R. Dahn, U. von Sacken, and C. A. Michal, *Solid State Ionics*, **44**, 87 (1990).
35) M. G. S. R. Thomas, W. I. F. David, and J. B. Goodenough, *Mater. Res. Bull.*, **20**, 1137 (1985).
36) G. G. Amatucci, J. M. Tarascon, and L. C. Klein, *J. Electrochem. Soc.*, **143**, 1114 (1996).
37) A. K. Barker, R. Pynenburg, R. Koksbang, and M. Y. Saidi, *Electrochim. Acta*, **41**, 2481 (1996).
38) S. Lunell, A. Stashans, L. Ojamäe, H. Lindström, and A. Hagfeldt, *J. Am. Chem. Soc.*, **119**, 7374 (1997).
39) A. K. Rappe, C. J. Casewit, K. S. Colwell, W. A. Goddard, III, and W. M. Skiff, *J. Am. Chem. Soc.*, **114**, 10024 (1992).
40) "Cerius^2, Version 3.0," Molecular Simulations Inc., San Diego (1997).
41) A. K. Rappe and W. A. Goddard, III, *J. Phys. Chem.*, **95**, 3358 (1991).
42) C. Kittel, "Introduction to Solid State Physics," 6th ed, John Wiley & Sons, New York (1986), p. 606.
43) D. M. Heyes, *J. Chem. Phys.*, **74**, 1924 (1981).
44) N. Karasawa and W. A. Goddard, III, *J. Phys. Chem.*, **93**, 7320 (1989).
45) R. Hoffmann, *J. Chem. Phys.*, **39**, 1397 (1963).
46) G. Landrum, "YAeHMOP (Yet Another Extended Hückel Molecular Orbital Package), Version 2.0," (1997).
47) G. Nuspl, K. Yoshizawa, and T. Yamabe, *J. Mater. Chem.*, **7**, 2529 (1997).
48) R. D. Shannon, *Acta Crystallogr., Sect. A*, **A32**, 751 (1976).
49) A. Guinier and R. Jullien, "The Solid State, From Superconductors to Alloys," Oxford University Press, Oxford (1989).
50) R. J. Borg and G. J. Dienes, "The Physical Chemistry of Solids," Academic Press, San Diego (1994).
51) A. N. Cormack and Y. Cao, *Mol. Eng.*, **6**, 183 (1996).